

Experimental and numerical studies for the forming groove and separating groove design in slit rolling process[†]

D. H. NA, S. H. Cho and Y. Lee*

Department of Mechanical Engineering, Chung-Ang University, Seoul, 156-756, Korea

(Manuscript Received March 6, 2011; Revised May 30, 2011; Accepted May 30, 2011)

Abstract

This paper presents a design method of the forming groove-to-separating groove rolling sequence used in slit rolling process. Based on the equivalent rectangle approximation, we have designed the forming groove which produces a peanut-shaped cross section via rolling from workpiece with an inlet (incoming) square cross section. The separating groove is designed by lowering its width and height in the ratio of 1:3 for the given reduction ratio. With the forming groove and separating groove designed by the proposed design method, we have performed a pilot rolling test at high temperature (around 1000°C) using low carbon (0.1%C) steel and have also carried out finite element analysis to examine the expansibility of the proposed design method. The Results reveal that if the ratio of the roll diameter over the side length of a square is in the range of 4.0 ~ 8.0, the design method proposed in this study can be systematically applied to design the forming groove-to-separating groove without relying on in-house databases and/or on-site experience.

Keywords: Slit rolling; Forming groove; Separating groove; Groove design method

1. Introduction

The term “slitting” dates back to the days of saw mills when logs would be cut into smaller sections lengthwise using straight or circular blades. In the steel manufacturing process, slitting is an operation in which a large cross section of metal is cut into smaller sections. For example, a coil of steel sheet is cut down into a number of steel sheets with narrower width.

The slit rolling operation has been used in manufacturing the deformed bar or rod. Two, three or even four deformed bars (or rods) can be simultaneously produced from a billet using a set of specially designed roll grooves to make mass productivity. After a billet is processed through the roughing mill at a high temperature (above 1000°C), the billet becomes a workpiece (material) with square cross section. This workpiece with a square cross section is delivered to slitting process which consists of three stages. (See Fig. 1) In the first stage, the forming groove alters an inlet (incoming) square cross section into a peanut-shaped cross section via rolling since the square cross section is to be bisected lengthwise later. In the second stage, the middle region of the peanut-shaped cross section becomes very thin by the separating groove as if two false round sections are connected. The thin region which

connects both sides of the false round section will be referred to as the ‘connector’ hereafter. In the third stage, the slitting rolls located at the rear of the separating groove split the connector lengthwise by applying a diagonal pressure to two false round sections. (See Fig. 2) Consequently, a square section is divided into two false round sections. If higher productivity is required, the slitting procedure can be repeated twice or three times. The design of the forming groove and separating groove is very important in slit rolling process since it affects the design of the oval groove and round groove, which should be positioned in that order after the forming groove-to-separating groove rolling.

Mróz used finite element method to estimate the effect of the shape of the separating groove on the roll force and on the distribution of roll wear [1]. But the research remained at numerical analysis stage. Stefanik et al. performed finite element analysis to examine the influence of roll speed variations (3, 6 and 9 m/s) on the distributions of the stress and strain at the connector [2]. They computed the distribution of the material’s specific plastic deformation energy and discussed its applicability to FE simulation of failure at the connector. Mróz et al. studied the relation between the roll and material contact length in the slitting process and used the Cockcroft-Latham criterion to simulate the rupture of the connector using finite element method [3, 4].

Previous studies focused on establishing a failure criterion at the connector and computing the roll force, the wear and the

[†] This paper was recommended for publication in revised form by Editor Maenghyo Cho

*Corresponding author. Tel.: +82 2 824 5256, Fax.: +82 2 814 9476

E-mail address: ysl@cau.ac.kr

© KSME & Springer 2011

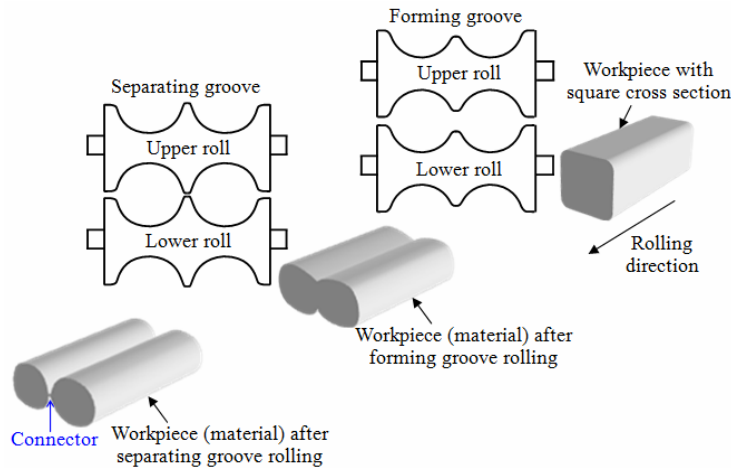


Fig. 1. The forming groove alters an inlet square cross section into a peanut-shaped cross section via rolling. Separating groove thins the middle region of the peanut-shaped cross section. The slitting rolls located at the rear of the separating groove bisect the workpiece lengthwise.

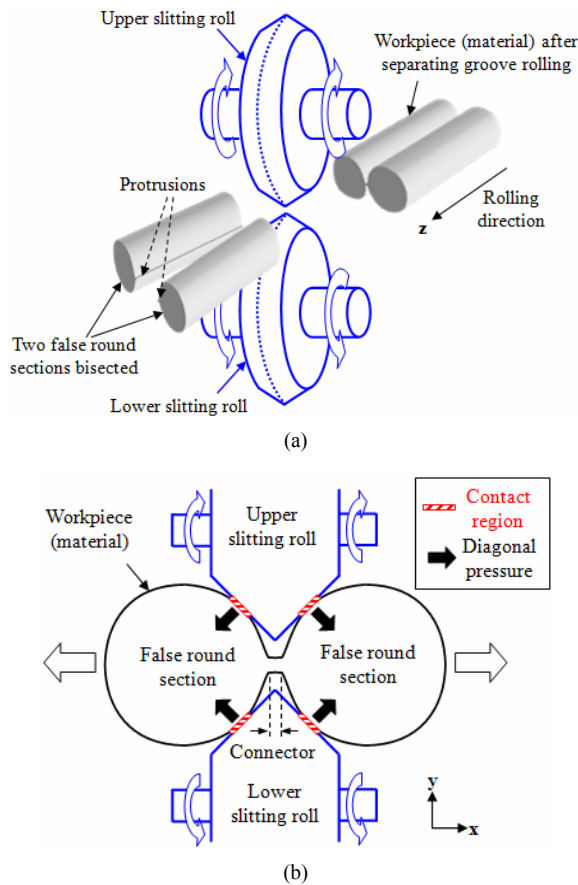


Fig. 2. (a) A schematic diagram of slitting process; (b) Slitting roll applies diagonal pressures to the contact regions so that two false round sections are bisected. An appropriately sized protrusion remains at the surface of the false round section after bisecting.

torque of the separating groove. No work for the design method of the forming groove and separating groove has been reported so far. To the author’s best knowledge, the forming groove and separating groove have been designed by the ex-

perienced groove designers in production-site. Hence the design method becomes a central issue in terms of technical progress in slit rolling process. It is the purpose of this paper to propose a systematic design method for those grooves.

In the present study, we have proposed a systematic design method for the forming groove and separating groove based on the equivalent rectangle approximation. Using the forming groove, separating groove designed and low carbon (0.1%C) steel, we have performed a pilot rolling test at a high temperature (around 1000°C) to demonstrate the validity of the proposed design method and have also carried out finite element analysis to investigate its expansibility.

2. Design method of the forming groove-to-separating groove

In what follows, the design method of the forming groove and separating groove for the cases in which the inlet (incoming) cross sectional shape is square is explained in detail. The design aim of these grooves is ultimately to produce two false round cross sections from a square cross section. The proposed design method is purely geometrical. The work rolls are assumed to be rigid and metallurgical effect such as oxide scaling on the material surface during hot rolling is not considered.

2.1 Design of the forming groove

Basic design:

Design of the forming groove is definitely related with the dimension of an inlet (incoming) square cross section. Considering the forming groove deforms the inlet square cross section into a peanut-shaped cross section, we first transform the inlet square cross section into a rectangular cross section whose ratio over the equivalent width to equivalent height should be slightly greater than 2.0 so that two false round cross sections including the connector region are produced later. Hence, we apply the equivalent rectangle approximation

method to the inlet square cross section. Fig. 3 illustrates the equivalent rectangle approximation applied to the inlet square cross section. The inlet square cross sectional area A_0 remains unchanged during transformation. The equivalent width W_{eq} is as follows:

$$W_{eq} = \frac{A_0}{0.7B_0} \quad (1)$$

Since the multiplication of W_{eq} and H_{eq} should be equal to A_0 , the equivalent height H_{eq} may have a form

$$H_{eq} = 0.7B_0 \quad (2)$$

where B_0 is the breadth of inlet square section. The thermal expansion caused by the high temperature and the area loss due to the corner radius of the square cross section was considered in the value of B_0 . In this way, the ratio of W_{eq} over H_{eq} becomes about 2.02. This confirms that the equivalent width W_{eq} and height H_{eq} are set properly.

Next, we determine the magnitude of design parameters of the forming groove shown in Fig. 4. W_{fm} and H_{fm} denote the width and height of the forming groove, respectively. If the

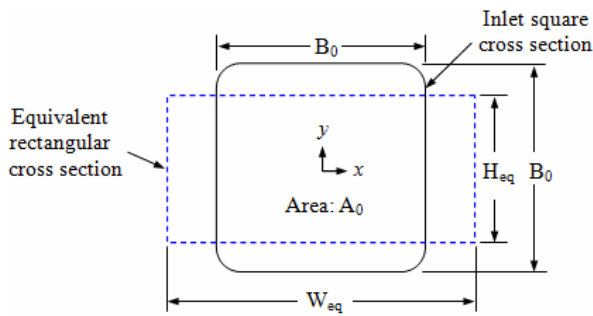


Fig. 3. Applications of the equivalent rectangle approximation to an inlet (incoming) square cross section. The solid line indicates the inlet square cross section and the dashed line indicates an equivalent rectangular cross section.

width and height of the forming groove are assumed to be the same with the width and height of the equivalent rectangle transformed from the inlet square cross section, we can determine W_{fm} and H_{fm} by setting

$$W_{fm} = W_{eq} \text{ and } H_{fm} = H_{eq} \quad (3)$$

Detail design:

D_{fm} , i.e., the distance between the centers of two false round sections should always be larger than $(W_{fm} - H_{fm})$. In addition, D_{fm} should be a function of W_{fm} and H_{fm} because D_{fm} is related to the magnitude of the false round sections. Thus, D_{fm} can then be expressed as follows:

$$D_{fm} = \gamma (W_{fm} - H_{fm}) \quad (4)$$

where a parameter γ is a correction coefficient greater than 1.0. If the value of γ is much greater than 1.0, the width of the connector becomes so long that the false round sections have a large size of protrusions at the surface of the false round section following slitting. (See Fig. 2(a)) A large size of protrusions become surface defects in the course of the oval groove and round groove rolling following the slitting process. If the value of γ is very close to 1.0, two false round sections are so close each other that their sectional shape after slitting might not be a false round anymore because of abnormal high pressure at the contact area of material and slitting rolls (See Fig. 2(b)). In this study, we choose $\gamma = (W_{fm} / H_{fm} - 1)$. Therefore, the final form for D_{fm} is

$$D_{fm} = \left(\frac{W_{fm}}{H_{fm}} - 1 \right) (W_{fm} - H_{fm}) \quad (5)$$

The interval between two circles C_{fm} is calculated as follows:

$$C_{fm} = D_{fm} - H_{fm} \quad (6)$$

The coordinates of the points O_{fm1} and O_{fm2} are then $(-D_{fm}/2,$

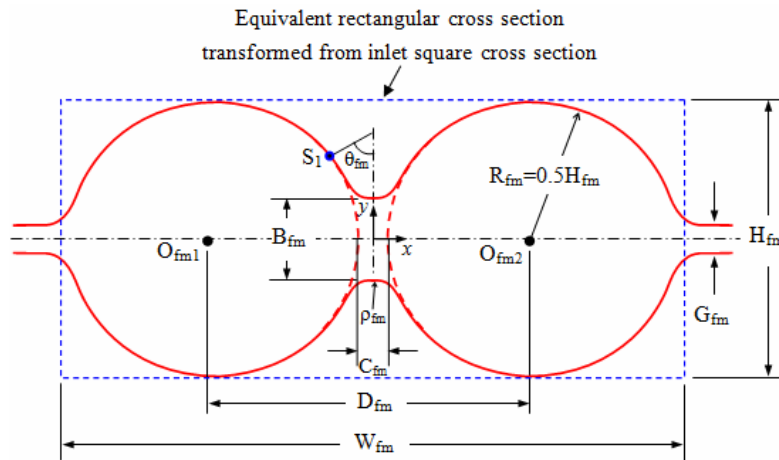


Fig. 4. A front view of the forming groove and its design parameters.

Table 1. The values of design parameters used for the forming groove (in mm). Descriptions of the parameters are given in Fig. 4.

Design parameter	Specimen size		
	20 × 20	30 × 30	40 × 40
W_{fm}	28.74	43.13	57.50
H_{fm}	14.21	21.32	28.42
D_{fm}	14.86	22.31	29.76
C_{fm}	0.65	0.99	1.34
B_{fm}	4.00	6.75	10.00
ρ_{fm}	1.00	1.60	2.34
θ_{fm}	68.33°	65.87°	63.67°
G_{fm}	3.78	4.27	5.73

0) and $(D_{fm}/2, 0)$.

When we determine the value of B_{fm} , we have to consider the biting angle limit because B_{fm} is dependent on it. In the case of the tandem rolling process, the biting angle limit is higher than the theoretical biting angle, i.e., $\alpha(=\tan^{-1}\mu)$. μ denotes the mean Coulomb friction coefficient at the interface of the material and the work roll. This is because the material being deformed at the previous groove, i.e., the square groove, yields a significant thrust force which pushes the material into the forming groove. The range of theoretical biting angle is $16.7^{\circ} \sim 21.8^{\circ}$ when the mean Coulomb friction coefficient is in the range of 0.3 ~ 0.4. Thus, B_{fm} is set to about 20 ~ 25% of B_0 .

The corner radius ρ_{fm} is given to reduce inhomogeneous metal flow during rolling and subsequently decreases roll wear at the corner region. Hence, the small value of the corner radius is preferred. In general, ρ_{fm} is set to be about equal to the C_{fm} determined by Eq. (6). θ_{fm} is a relief angle which plays a role in smoothing the metal flow near the connector region. Once B_{fm} and ρ_{fm} are known, the value of θ_{fm} can be easily determined using Eq. (7)

$$\theta_{fm} = \cos^{-1} \left(1 - \frac{S_1 - 0.5B_{fm}}{\rho_{fm}} \right). \quad (7)$$

S_1 denotes the value of y-coordinate of a point where the radius of curvature ρ_{fm} and the radius of R_{fm} meet each other. Using Eq. (1) through Eq. (7), we can compute the values of design parameters of the forming groove for the cases in which the sizes of the inlet square cross section are 20 mm, 30 mm and 40 mm in breadth (width). The results are shown in Table 1.

2.2 Design of the separating groove

Basic design:

Fig. 5(a) illustrates that the forming groove and separating groove are piled up to compare these two groove shapes. It shows the difference and similarity between these two grooves

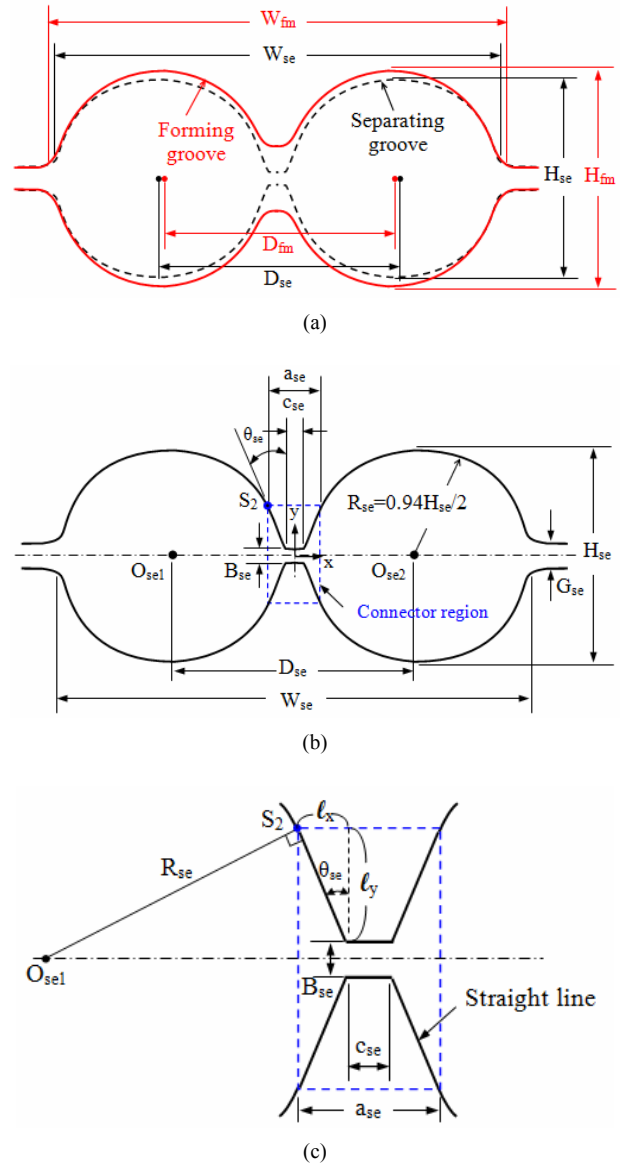


Fig. 5. (a) The case that the forming groove and separating groove are overlapped; (b) A front view of the separating groove and its design parameters; (c) Magnification of the connector and its neighboring region. B_{se} and c_{se} denote the thickness and width (length) of the connector, respectively.

straightforwardly. The shape of the forming groove is similar to a peanut, but the separating groove looks like two conjoined circles. The width and height of the separating groove are smaller than those of the forming groove. The shapes of the connector and its neighboring region are different.

Fig. 5(b) shows the design parameters of the separating groove. From the forming groove to the separating groove, about 8% of reduction ratio is usually assigned [3]. We make use of it to determine the width and height of the separating groove. The reduction ratio is assumed to be shared out to a decrease at the rate of 1:3. That is to say that the width of the separating groove equals that of the forming groove which is

Table 2. The values of design parameters used for the separating groove (in mm). Descriptions of the parameters are given in Fig. 5(b).

Design parameter	Specimen size		
	20×20	30×30	40×40
W_{se}	28.17	42.27	56.35
H_{se}	13.36	20.04	26.71
D_{se}	15.14	22.74	30.33
B_{se}	0.7	0.9	1.0
θ_{se}	20.0	20.0	20.0
c_{se}	1.4	1.8	2.0
a_{se}	2.80	3.63	4.79
G_{se}	1.98	2.67	4.00

reduced by 2% and the height of the separating groove equal to that of the forming groove that is reduced by 6%. Hence, the width W_{se} and height H_{se} of the separating groove are

$$W_{se} = (1-0.02)W_{fm} = 0.98W_{fm} \quad (8a)$$

$$H_{se} = (1-0.06)H_{fm} = 0.94H_{fm} \quad (8b)$$

where W_{fm} and H_{fm} represent the width and height of the forming groove.

Detail design:

Since the cross section rolled out of the forming groove is fed in the separating groove without 90 degree turning, we can adopt the concept applied in Eq. (4) to determine D_{se} , i.e., the distance between the centers of two false round sections in Fig. 5(a) and (b). D_{se} is then expressed as follows:

$$D_{se} = \gamma(W_{se} - H_{se}) \quad (9)$$

where $\gamma = \left(\frac{W_{fm}}{H_{fm}} - 1 \right)$.

Fig. 5(c) illustrates a magnification of the connector and its neighboring region. The parameter a_{se} is highly influenced by the sharpness of slitting roll edge B_{se} , i.e., the thickness of the connector. The value of B_{se} should be as small as possible so that the connector is easily split by the slitting rolls. In general, B_{se} and θ_{se} are set to approximately 0.7 ~ 1.0 mm and 20 degrees. c_{se} is set to about 1.5 ~ 2.0 times of the value of B_{se} . S_2 indicates a point where a relief angle θ_{se} starts. With the values of B_{se} , θ_{se} and c_{se} , we can determine the coordinate of $S_2(l_x, l_y)$ along these lines

$$l_y = R_{se} * \sin\theta_{se} - \frac{B_{se}}{2} \quad (10a)$$

$$l_x = \frac{\sin\theta_{se}}{\sin(90 - \theta_{se})} l_y \quad (10b)$$

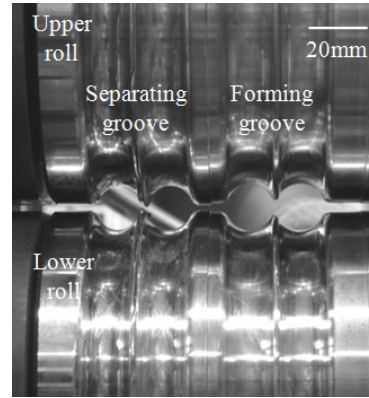


Fig. 6. The forming groove and separating groove used in the rolling test.

Thus, a_{se} is calculated as follows:

$$a_{se} = c_{se} + 2l_x \quad (11)$$

Using Eq. (8) through Eq. (11), we can calculate the values of design parameters of the separating groove when the inlet square cross section is 20 mm, 30 mm and 40 mm in breadth (width). The results are shown in Table 2.

3. Experimental

Based on all design parameters of the forming groove and separating groove, we have machined the roll grooves and have performed a pilot rolling test. Fig. 6 shows the forming groove and separating groove used in the rolling test.

3.1 Material, rolling mill and grooves

The material used in this study was a low carbon (0.1%C) steel. The material was obtained in the form of a square as-cast billet (160 mm×160 mm). A specimen, 30 mm square and 250 mm length, was machined. The corner radius of the specimen cross section was 3 mm. A single-stand two-high laboratory rolling mill was employed, driven by an 11kW constant torque DC motor. DCI (Ductile Casting Iron) roll with diameter of 160 mm was used. Entry guides were installed in the front of each roll groove to minimize the lateral bending of the specimen during rolling. The rolling speed was approximately 0.27m/s.

3.2 Rolling test procedure

The specimen was heated in a reheating furnace at 1100°C for 20 minutes to ensure a homogenous temperature distribution. Before rolling, the surface temperature was measured using a high temperature pyrometer. The square specimen was first rolled in the forming groove when the surface temperature reached 1000°C. The rolled specimen was put back into the reheating furnace. Fifteen minutes later, the rolled specimen was then rolled in the separating groove at a surface tem-

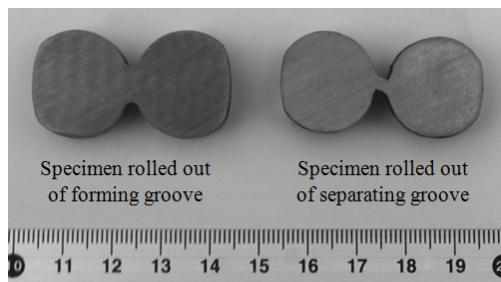


Fig. 7. Cross sectional shapes of the specimen rolled out of the forming groove and separating groove. The breadth of the inlet square specimen is 30 mm.

perature of 1000°C. No lubricant was used in the rolling test. The specimen rolled from the forming groove and separating groove was cooled in air to room temperature. After cooling, 10 mm-thick cross sections were obtained by cutting down at the middle of the rolled specimen. We then obtained the coordinates of its surface profile and computed its cross sectional area.

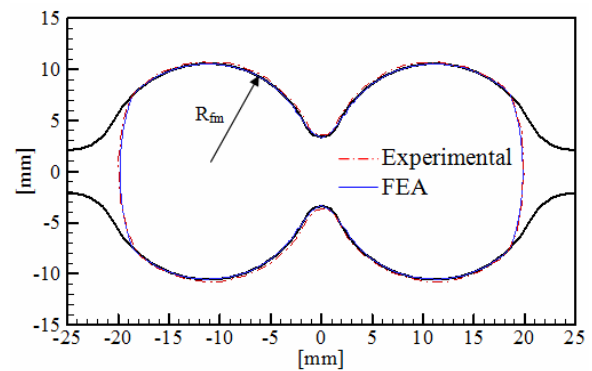
4. Results and discussion

4.1 Square cross section-30 mm in width

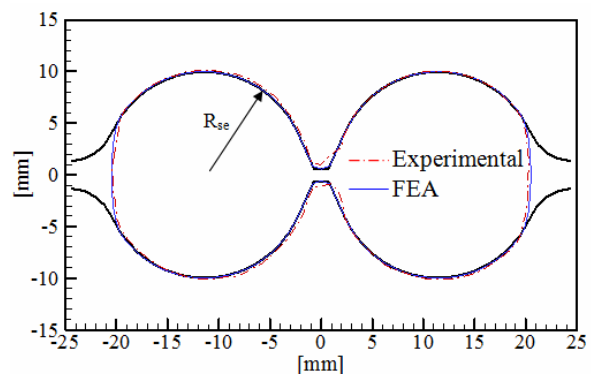
Fig. 7 shows the cross sectional shapes of the specimen after rolling test. The breadth of the inlet square specimen is 30 mm. The cross sectional shape rolled out of the separating groove is somewhat unbalanced since the upper and lower separating grooves were slightly dislocated from the bilateral symmetry during rolling. This would not be good for mass production in the industry. However, this can be avoided if the separating groove shape has vertical symmetry.

Fig. 8 compares the exit cross sectional shapes measured with the shapes calculated by finite element method. Finite element analysis was conducted using ABAQUS (Ver. 6.9–1). The explicit time integration method was employed and element type used for the specimen was C3D8R (8-node linear brick, reduced integration with hourglass control). Coulomb friction coefficient, 0.30 was used [5, 6]. The number of specimen elements used is 18,000 and roll elements are 5,000. The boundary conditions employed in FE simulation are the same conditions that Byon et al. adopted for the analysis of hot rod rolling process [7]. The differences in the exit cross sectional areas are 2.3% for the forming groove and 0.2% for the separating groove, respectively. Thus, the FE analysis in the forming groove and separating groove rolling is proved to be valid.

The calculated exit cross sectional areas after the forming groove (Fig. 8(a)) and separating groove rolling (Fig. 8(b)) are 675.9 mm² and 622.9 mm², respectively. It indicates that the reduction ratio from the forming groove to the separating groove is 7.84%. This result verifies the usefulness of the proposed design method since we assumed about 8% of reduction ratio at the forming groove-to-separating groove rolling sequence. (See basic design in Section 2.2)



(a)



(b)

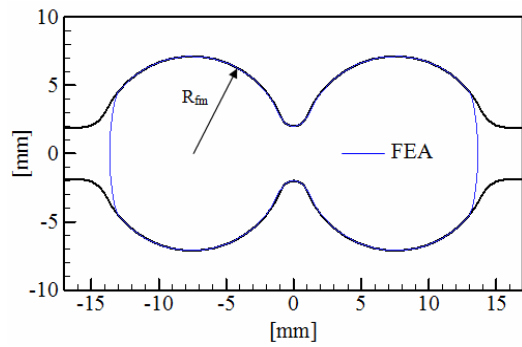
Fig. 8. Measured exit cross sectional shapes and computed ones when a square specimen with 30 mm in width was rolled. R_{fm} and R_{se} denote the radius of forming groove and that of separating groove, respectively: (a) Forming groove; (b) Separating groove.

In slitting process, the connector (the thin region which connects both sides of the two false round sections) is bisected lengthways by the slitting rolls positioned at the rear of the separating groove. (See Fig. 2(a)) The two bisected false round sections are then rolled in an oval groove-to-round groove rolling sequence in the form of two separate deformed bars (or rods), respectively. Therefore, if the separating groove was properly designed, half of the exit cross sectional area produced by the separating groove should be equal to a circular area ($=\pi R_{se}^2$) with a radius of R_{se} (See Fig. 5(b)). Fig. 8(b) shows that the difference between half of the exit cross sectional area and the circular area with a radius of R_{se} was 0.72%, indicating that the design method proposed in this study was successful.

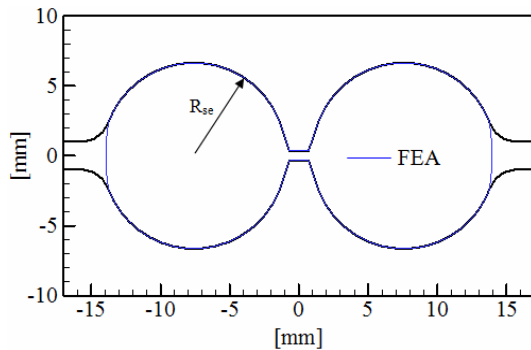
As a result of this success, we were encouraged to change the size of the inlet square dimension to assess the expansibility of the proposed design method. In this study, we used finite element method to do it when the size of the inlet square dimension varies.

4.2 Square cross section-20 mm and 40 mm in width

Fig. 9 show the computed exit cross sectional shapes when



(a)



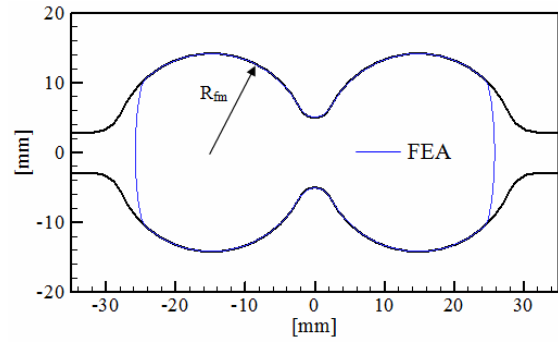
(b)

Fig. 9. Computed exit cross sectional shapes when a square specimen with 20 mm in width was rolled. R_{fm} and R_{se} denote the radius of forming groove and that of separating groove, respectively: (a) Forming groove; (b) Separating groove.

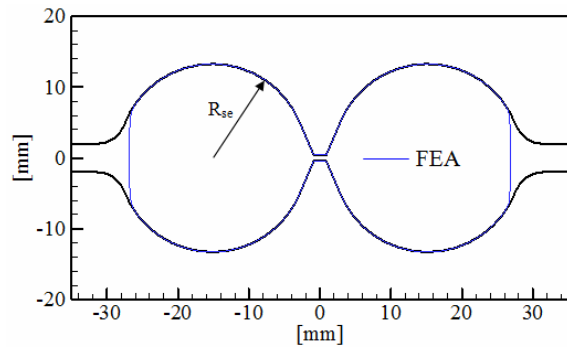
a 20 mm-square specimen was rolled in the forming groove and separating groove. In Fig. 9(b), the difference between half of the computed exit cross sectional area rolled out of the separating groove and the circular area with a radius ($=\pi R_{se}^2$) of R_{se} is 0.16%. It is deduced that we can use the proposed design method when the inlet square dimension is reduced from 30 mm to 20 mm.

Fig. 10 illustrates the computed exit cross sectional shapes when a square specimen with 40 mm in width was rolled in the forming groove and separating groove. In Fig. 10(b), the difference between half of the computed exit cross sectional area and the circular area with a radius of R_{se} is 1.70%, which is slightly larger than for the other cases, i.e., 20 mm and 30 mm square specimens. This is because the radius of R_{fm} and R_{se} calculated is slightly larger than necessary and a lower ratio of the roll diameter over the side length of a square leads to a lesser spread of material during rolling. Note that the side length of the inlet square was increased from 30 mm to 40 mm while the roll diameter remained fixed.

The FEA results (Figs. 8–10) imply that the proposed design method can be applied to the design of the forming groove and separating groove without performing a rolling test, which usually requires a high cost and a lot of time. The proposed design method might be useful when the ratio of the roll diameter (160 mm) over the square height (breadth) on a side is



(a)



(b)

Fig. 10. Computed exit cross sectional shapes when a square specimen with 40 mm in width was rolled. R_{fm} and R_{se} denote the radius of forming groove and that of separating groove, respectively: (a) Forming groove; (b) Separating groove.

in the range of 4.0 ($=160 \text{ mm}/40 \text{ mm}$) \sim 8.0 ($=160 \text{ mm}/20 \text{ mm}$). In case that the ratio is below 4.0, we can still use the proposed design method if we reduce the width and height of the separating groove through FE simulation.

5. Concluding remarks

This study has proposed a design method based on the equivalent rectangle approximation to design the forming groove and separating groove, which are very critical in slit rolling process where the inlet (incoming) cross sectional shape is square. We have performed a pilot hot rolling test to validate the effectiveness of the proposed design method and have also carried out finite element analysis as well to investigate the expansibility of the proposed design method. The conclusions are summarized as follows:

If the ratio of the roll diameter over the side length of a square is in the range of 4.0 \sim 8.0, the design method proposed in this study works well. It can be used to design the forming groove-to-separating groove without relying on in-house databases and/or on-site experience. The proposed design method can be expanded to a wider range of ratio (the roll diameter over the square dimension) if we simulate properly the forming groove and separating groove rolling using finite element method.

Acknowledgment

This research was supported by the Chung-Ang University Freshman Academic Record Excellent Scholarship Grants in 2010.

Reference

- [1] S. Mróz, Examination of the effect of slitting roller shape on band slitting during the multi slit rolling process, *Journal of Achievements in Materials and Manufacturing Engineering*, 26 (2) (2008) 167-170.
- [2] A. Stefanik, Slitting criterion for various rolling speeds in MSR rolling process, *Journal of Achievements in Materials and Manufacturing Engineering*, 27 (1) (2008) 91-94.
- [3] S. Mróz, A. Stefanik and H. Dyja, The application of the inverse method for determination of slitting criterion parameter during the multi slit rolling (MSR) process, *Journal of Materials Processing Technology*, 177 (1) (2006) 493-496.
- [4] M. G. Cockroft and D. J. Latham, A simple criterion of fracture for ductile metals, *Journal of the Institute of Metals*, 96 (1968) 33-39.
- [5] L. S. Bayoumi, Y. Lee and H. J. Kim, Effect of roll gap change of oval pass on interfacial slip of workpiece and roll pressure in round-oval-round pass rolling sequence, *Journal of Mechanical Science Technology*, 16 (4) (2002) 492-500.
- [6] W. J. Kwak, Y. H. Kim, J. H. Lee and S. M. Hwang, A precision on-line model for the prediction of roll force and roll power in hot-strip rolling, *Metallurgical and Materials Transactions A*, 33 (10) (2002) 3255-3272.
- [7] S. M. Byon, D. H. Na and Y. Lee, Effect of roll gap adjustment on exit cross sectional shape in groove rolling-Experimental and FE analysis, *Journal of Materials Processing Technology*, 209 (9) (2009) 4465-4470.



Doohyun Na received his bachelor's degree in 2007 and Master's degree in 2009 in Mechanical Engineering from Chung-Ang University. His research area is mainly the thermal fatigue crack growth behavior of roll in hot strip rolling. He is currently doing his Ph.D in the Department of Mechanical Engineering, Chung -Ang University, Seoul, Korea.



Sangheum Cho received the Bachelor's degree in Mechanical Engineering from Chung-Ang University, Korea, in 2010. Sangheum Cho, he is currently a M.S. student in Chung-Ang University, Seoul, Korea.



Youngseog Lee received the B.S. in Mechanical Engineering from Pusan National University, Korea, in 1989. He then received the M.S. and Ph.D. degrees from Case Western Reserve University, Cleveland, Ohio, USA, in 1992 and 1997, respectively. Until 2003, he worked as a researcher at POSCO Technical Research Laboratories, Pohang, Korea. He is currently an Associate Professor in the Department of Mechanical Engineering, Chung-Ang University, Seoul, Korea. He is interested in computational fracture mechanics and hot rolling process.